Chemosphere 206 (2018) 398–404

Contents lists available at ScienceDirect

Chemosphere

journal homepage: www.elsevier.com/locate/chemosphere

Degradation of hydraulic fracturing additive 2-butoxyethanol using heat activated persulfate in the presence of shale rock

Katherine E. Manz [a, b], Kimberly E. Carter [a, b, *]

[a] University of Tennessee/Oak Ridge National Laboratory Bredesen Center, University of Tennessee, Knoxville, TN 37996, USA
[b] Department of Civil and Environmental Engineering, University of Tennessee, Knoxville, TN 37996, USA

HIGHLIGHTS

- 2-BE (HF chemical) rapidly oxidizes via heat activated persulfate with iron present.
- Shale rock addition slows 2-BE degradation, despite increasing iron concentrations.
- During 2-BE degradation, persulfate may react with shale causing metal dissolution.

ARTICLE INFO

Article history:
Received 7 February 2018
Received in revised form
18 April 2018
Accepted 1 May 2018
Available online 4 May 2018

Handling Editor: Keith Maruya

Keywords:
2-Butoxyethanol
Hydraulic fracturing
Shale rock
Persulfate
TDS

ABSTRACT

Changes in fluid composition during hydraulic fracturing (HF) for natural gas production can impact well productivity and the water quality of the fluids returning to the surface during productivity. Shale formation conditions can influence the extent of fluid transformation. Oxidizers, such as sodium persulfate, likely play a strong role in fluid transformation. This study investigates the oxidation of 2-butoxyethanol (2-BE), a surfactant used in HF, by sodium persulfate in the presence of heat, pH changes, Fe(II), and shale rock. Increasing temperature and Fe(II) concentrations sped up 2-BE oxidation, while pH played little to no role in 2-BE degradation. The presence of shale rock impeded 2-BE oxidation with increasing shale concentrations causing decreasing pseudo-first-order reaction rate constant to be observed. Over the course of reactions containing shales, dissolved solids were tracked to better understand how reactions with minerals in the shale impact water quality.

1. Introduction

Extracting oil and natural gas from unconventional shale reservoirs requires HF with high volumes of water mixed with chemical additives (Gregory et al., 2011; Chen and Carter, 2016). Chemical additives include surfactants and oxidizing breakers that likely transform during the fracturing process (Thurman et al., 2014; Kahrilas et al., 2016). Transformation of additives and shale may impact the flowback and produced water quality that returns to the surface during natural gas production.

HF wastewater spills are a concern due to potential contamination of water aquifers. While many chemicals have been identified in hydraulic fracturing flowback and produced fluids, the transformed fluids are the source of pollution when spills occur. Surfactants are consistently found in HF waters (Kahrilas et al., 2016). 2-BE is a commonly identified surfactant found in HF additives including the foaming agent, Revert Flow (Stringfellow et al., 2014; Llewellyn et al., 2015; Rogers et al., 2015, 2017; DiGiulio and Jackson, 2016; Manz and Carter, 2016; Manz et al., 2016; Marcon et al., 2017). Revert Flow improves production by decreasing surface tension, thus preventing water blocking during the HF process. While the harsh physical conditions downhole may stimulate organic additive transformation, HF operators also use strong oxidizing agents such as persulfate salts (Gaillard et al., 2013; Stringfellow et al., 2014; Paukert Vankeuren et al., 2017). Persulfate has the potential to speed up and enhance transformations, therefore; persulfate is a key component to understanding how additives transform during the HF treatment of a well.

* Corresponding author. University of Tennessee/Oak Ridge National Laboratory Bredesen Center, University of Tennessee, Knoxville, TN 37996, USA.
E-mail address: kcarte46@utk.edu (K.E. Carter).

https://doi.org/10.1016/j.chemosphere.2018.05.007
0045-6535/

Addition of shale to persulfate reactions in the HF environment has not been previously investigated. Persulfate activation through increased formation temperatures and pressures has been previously investigated by the authors (Manz and Carter, 2017). As persulfate activation was observed under HF conditions (Manz and Carter, 2017), the shale constituents may impede or enhance the activation. For example, shale contains minerals that contain iron, which may activate persulfate (Ahmad et al., 2010) and enhance oxidation of additives. Minerals found in shale include pyrite, hematite, goethite, and limonite (Grim and Rowland, 1944; Marcon et al., 2017). Shale also contains minerals, such as chlorite and gypsum (Phan et al., 2018; Marcon et al., 2017), which may prevent oxidation of additives because these minerals contain carbonates (Liang et al., 2006).

The objective of this study is to address the potential persulfate activation using shale rock and the impact it has on 2-BE degradation and water quality. Fluid conditions that mimic those used during a fracture, including temperature, pH, iron, and shale rock, are systematically introduced. Further impacts persulfate usage has on HF water quality are evaluated through quantification of metals leached into solution during shale-activated reactions. Determination of 2-BE oxidation reactions with persulfate in the presence of shale will enable a better understanding of the impacts persulfate utilization has on flowback and produced water quality.

2. Experimental

2.1. Chemicals

Solutions were prepared using deionized water (Milli-Q Plus purification system, Darmstadt, Germany). Chemical used, including 2-BE (95%), Optima grade dichloromethane, ferrous sulfate (>99%), hydrochloric acid (35–38%), sodium persulfate (>98%), TraceMetal™ grade nitric acid, sodium persulfate (>98%), sodium bicarbonate (>99%), potassium iodide (>99%), and SPEX CertiPrep™ calibration standard 2 without mercury (5% nitric acid), were purchased from Fisher Scientific (Pittsburgh, PA 15275, USA). Revert Flow (RF) was received from Weatherford International (Houston, Texas, USA).

2.2. Shale rock

WV-7 shale rock used in this study was obtained from the Marcellus shale play at a depth of 6621.1 m (West Virginia Geological Survey, Morgantown, WV 26508, USA). The shale was crushed with a mortar and pestle and sieved to a mean diameter of 1.00–2.00 mm using No. 10 and 18 sized meshes. Bulk shale minerology was determined using X-Ray diffraction (XRD) and verified using acid digestion and inductively coupled plasma optical emission spectrometry (ICP-OES) analysis. Diffraction patterns were collected using a Panalytical Empyrean XRD with Cu source (Almelo, Netherlands) and ICP-OES data was collected with a ThermoFisher Scientific iCAP DUO 7400 (Waltham, MA 02451). Fig. S1 in the supporting information (SI) displays the resulting diffractagram of the unreacted WV7 shale and Fig. S2 displays the ICP digestions results. Bulk minerology of the shale is listed in Table 1 and contained calcite, dolomite, muscovite-2M1, rubidium zinc silicon oxide, pyrite, and quartz. Microscope observations were made using a Zeiss scanning electron microscope (SEM) (model EVO-MA15) equipped with an Energy-dispersive X-ray (EDS) detector (Bruker, model X Flash 6130).

2.3. Batch oxidation experiments

In HF practices, surfactants are used in total concentrations ranging from 500 to 1800 mg L^{-1} (Stringfellow et al., 2014), while the HF additive supplier suggested RF concentration of 1 gallon RF per 1000 gallons water (Manz and Carter, 2016). RF was determined to be 1.0328 g mL^{-1} and contained 3.31 wt% 2-BE (Manz and Carter, 2016). Therefore, the 2-BE concentration in HF fluids may be as low as 34 mg L^{-1}. Solutions in this study contained 120 mg L^{-1} 2-BE for ease of measurement and were prepared 12 h prior to experiments, which allowed for overnight mixing in amber jars. Fe(II) concentrations used to activate persulfate ranged from 0 to 100 mg L^{-1}. Fe (II) was used because 2 + is the same oxidation state as the pyrite found in the WV7 shale rock. Acidic conditions such as those used in the industry, 0.012–15% (Ferrer and Thurman, 2015; Kekacs et al., 2015; Torres et al., 2016; Marcon et al., 2017), were achieved using 0.07% hydrochloric acid as listed by FracFocus (Manz and Carter, 2017). pH was measured with a Fisher Scientific Accumet XL600 benchtop pH meter (Pittsburgh, PA 15275, USA). Experiments were performed in triplicate using 250-mL volumes in capped 1-L amber borosilicate jars. The jars were placed in a shaking water bath (New Brunswick Scientific Co, Inc, Model G76, Edison, NJ USA) 12 h prior to experiment start at temperatures of 20, 35, 45, 55, and 65 °C. Experiments were spiked with a concentrated solution of stock sodium persulfate to a final concentration of 21 mmol L^{-1} to initiate experiments. Fracing fluids can return to the surface of the well from the first day after fluids are injected and may continue to flow out for several years following injection (Mouser et al., 2016). However, 2-BE was degraded much faster than this time frame. Therefore, experiments were carried out for 8 h, with the exception of experiments performed at 20, 35, and 45 °C because persulfate activation was slower at these temperatures than at higher temperatures. Samples were taken at designated times between 0 and 480 min in 10-mL volumes. Samples were immediately extracted for 2-BE (Manz and Carter, 2016) and analyzed for pH, TOC, and persulfate concentration. Mass balance calculations were performed to minimize sampling effects. Control experiments were performed without persulfate to account for the 2-BE oxidation at high temperatures and possible 2-BE absorption onto shale.

2.4. Sample analysis

2-BE concentration was determined using an Agilent 7890B gas chromatograph (GC) (Santa Clara, CA 95051) equipped with a splitter that connected to a 5977 A Mass Selective spectrometer (MS) and a flame ionization detector (FID), allowing simultaneous MS and FID analysis. The liquid-liquid extraction procedure and GC parameters have been previously described (Manz and Carter, 2016). In short, 3-mL of sample was pipetted into a scintillation vial containing 3-mL of methylene chloride and vortexed using a 115 V Mini Vortex Mixer (Fisher Scientific, Pittsburgh, PA 15275). The solution was separated using a 6-mL polypropylene syringe (Fisher Scientific, Pittsburgh, PA 15275) and the methylene chloride was collected in a separate vial. The extraction procedure was repeated three times. Calibration curves were made using known 2-BE concentration dissolved in methylene chloride. Extractions were repeated with hexane and chloroform to detect additional reaction byproducts as different compounds have different affinities for different solvents. The GC-MS-FID was operated in splitless mode and equipped with an Agilent 7963 auto-sampler and an Agilent J&W DB-1 (30-m x 0.25-mm ID x 0.25-μm film thickness) capillary column. Ultra-high purity helium (Airgas Corporation, Knoxville, TN 37921) was used as the carrier gas and maintained at 2.5 mL min^{-1}. Samples (2.5-μL injection volume) were analyzed in triplicate. The GC was held at an initial temperature of 40 °C for 4 min, and the temperature was ramped up 10 °C min^{-1} to 180 °C, and held at 180 °C for 3 min before ramping back down. The limit of detection of this method is 0.957 mg L^{-1} 2-BE

Table 1
WV7 shale minerology.

Mineral Name	Chemical Formula	Approximate Designation
Calcite	$CaCO_3$	Major
Dolomite	$MgCa(CO_3)_2$	Minor
Muscovite – 2M1	$KAl_2(Si_3Al)O_{10}(OH)_2$ w/Mg, Fe	Minor
Rubidium Zinc Silicon Oxide	Rb_2ZnSiO_3	Trace
Pyrite	FeS_2	Minor
Quartz	SiO_2	Major
Designation		
Major	>25%	
Minor	10-25%	
Trace	<10% clearly in sample	

(Manz and Carter, 2016).

Total Organic Carbon (TOC) was measured using a TOC-LCSH/CSN series standalone analyzer equipped with an ASI autosampler and a high sensitivity catalyst (Shimadzu, Kyoto, Japan). TOC standards were made using a known amount of 2-BE in 2.5% hydrochloric acid. TOC was determined using the difference between the total carbon (TC) and inorganic carbon (IC) concentrations.

A modified spectrophotometric/iodometric method was used to measure the persulfate anion(Kolthoff and Carr, 1953; Liang et al., 2008). Briefly, 166 g L^{-1} KI and 12 g L^{-1} $NaHCO_3$ were added to DI water and mixed until all components dissolved. Depending on the anticipated persulfate concentration, 20–50-μl of sample was added to a scintillation vial containing 2.5-mL of the KI/$NaHCO_3$ solution. The mixture reacted for 20 min and measured using a UV/Vis spectrophotometer (Thermo Fisher Scientific, Model Evolution 600 Madison, WI 53711, US) at the maximum wavelength of 352 nm. Standards were prepared by pipetting 20-μl of a 22-mM persulfate solution into 2.5, 3, 4, 5, and 7.5 mL aliquots of the KI/$NaHCO_3$ solution.

Metals leaching from the shale were measured using ICP-OES. Concentrations were determined by comparison to serial dilutions of a standard solution containing 10 mg L^{-1} of the following metals: Ag, Al, As, Ba, Be, Bi. Ca, Cd, Co, Cr, Cs, Cu, Fe, Ga, In, K, Li, Mg, Mn, Na, Pb, Rb, Se, Sr, Tl, U, V, and Zn.

2.5. Statistics

For all sample analysis, standard error (SE) of the data was calculated (equation in SI) and are represented by error bars in the Figures. Statistical analysis was performed using JMP Pro software from SAS, version 12.0.1 (Cary, NC 27516) to determine if the mean observed reaction rate constant for each experimental condition was significantly different from the other conditions tested. One-way analysis of variance (ANOVA) paired with a post-hoc Tukey-Kramer honest significant difference (HSD) test was used ($\alpha = 0.05$).

3. Results and discussion

3.1. Temperature effects

Fig. S3 (SI) displays the degradation of 2-BE in water at 20 °C without persulfate in an amber jar (pH 6). Previous studies have shown that 2-BE is susceptible to photo-degradation at 20 °C when experiments are performed in clear glassware (Minero et al., 1989; Manz and Carter, 2016). Fig. S3 shows little to no 2-BE degrades over 22,500 min (15.6 days), in the dark environment of the amber jar, which is similar to well-bore conditions. Fig. S4 shows the degradation of 2-BE with the addition of 21 mM persulfate at 20 °C in (a) and the pseudo-first-order plot in (b). Fig. S4b shows 65% of the initial 2-BE concentration degraded after 22,500 min. The plot of concentration versus time displayed a greater R^2 value then the plot of natural concentration versus time, which indicates that the reaction order with respect to 2-BE is pseudo zero-order at room temperature with a rate constant of 2.24×10^{-5} M s^{-1}. Fig. S5 displays the TOC, pH and persulfate concentration after 22,500 min. TOC and persulfate decreased by 22 and 15%, respectively, while the pH decreased from 6 to 3.06. The persulfate-induced oxidation of 2-BE at low temperatures suggests the persulfate anion may play a role in 2-BE degradation (Liang and Su, 2009). The persulfate reduction half-reaction is shown in Reaction 1. The direct oxidation of 2-BE by the persulfate anion is feasible as this strong oxidizing anion possesses a redox potential of 2.01 V (Tsitonaki et al., 2010).

$$S_2O_8^{2-} + 2e^- \rightarrow 2SO_4^{2-} \quad (1)$$

The oxidation of 2-BE at higher temperatures (35–65 °C) is shown in Fig. 1. The corresponding TOC, pH, and persulfate profiles are shown in Figure S6 (SI). The full-time scale for 2-BE, TOC, pH, and persulfate degradation at 35 and 45 °C is shown in Figure S7 and Figure S8 (SI), respectively. Both the 2-BE and persulfate degradation increased as temperature increased from 35 to 65 °C.

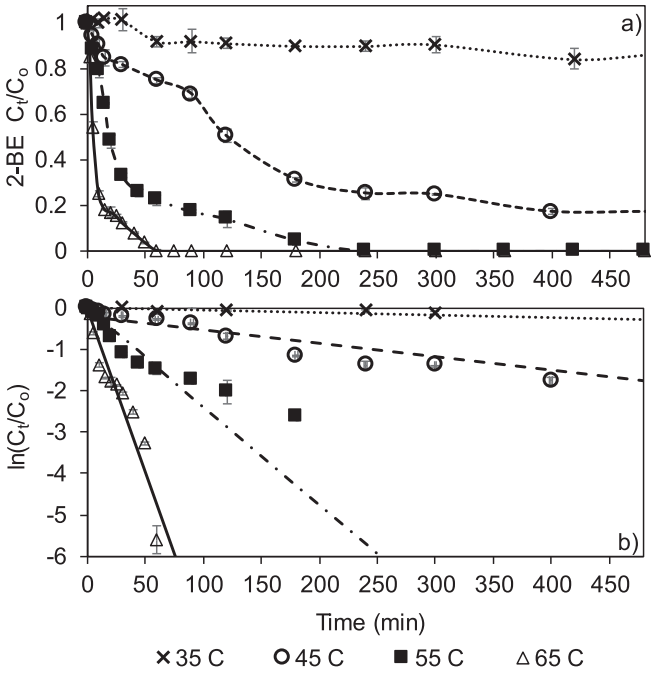

Fig. 1. 2-BE concentration profile as temperature increases shown in (a) and pseudo-first-order natural log plot versus time in (b) (initial sodium persulfate dose 21 mmol L^{-1}, initial pH 6). Error bars represent standard error. The limit of detection of the method used was 0.957 mg L^{-1} 2-BE.

These results were expected as increasing temperatures lead to persulfate activation, which increases production of sulfate radicals (Reaction 2) (House, 1962; Tsitonaki et al., 2010). As the temperature increases, more radicals are produced and these radicals may oxidize the 2-BE in solution. The sulfate radical reacts with water (Reaction 3) (Kolthoff and Miller, 1951; House, 1962; Herrmann et al., 1995), producing hydrogen ions and the observed pH drop. As shown in Fig. 1b, a pseudo-first-order rate model describes 2-BE oxidation well for higher temperatures. Table S1 summarizes the resulting reaction rate constants and half-lives. Values for $k_{obs,2BE}$ at 35, 45, 55, and 65 °C were 1.034×10^{-5}, 6.243×10^{-5}, 4.074×10^{-4}, and 1.312×10^{-3} s^{-1}, respectively. Fig. 2 shows the Arrhenius plot for the oxidation of 2-BE by all oxidants produced in thermal persulfate activation. The plot of natural log of k_{obs} versus the inverse temperature fit the Arrhenius model with $R^2 = 0.997$. The average activation energy was $146.95 \pm .44$ kJ mol^{-1}. The temperature dependence of this reaction is likely due to the persulfate decomposition and increased production of radicals.

$$S_2O_8^{2-} \rightarrow 2SO_4^{\cdot -} \quad (2)$$

$$SO_4^{\cdot -} + H_2O \rightarrow HO^{\cdot} + H^+ + SO_4^{2-} \quad (3)$$

As shown in Fig. 1, at 65 °C, 2-BE completely degrades within 50 min of the reaction. At 55 °C complete 2-BE degradation does not occur until 240 min. Since 2-BE degradation occurs more quickly at higher temperatures, this suggests that the persulfate was heat-activated to produce sulfate radicals as described in Reaction 2. Fig. S9 compares the persulfate disappearance at 55 °C with and without 2-BE present. Without 2-BE, the k_{obs} for persulfate activation is 3.53×10^{-6} s^{-1} at 55 °C, which agrees with values previously reported by House (4.55×10^{-6} s^{-1} at 56 °C) (House, 1962). With 2-BE, the $k_{obs,\ persulfate}$ value is 1.04×10^{-5} s^{-1} at 55 °C. The increasing persulfate disappearance with 2-BE in solution suggests that the radicals produced by thermal persulfate activation degrade 2-BE while direct oxidation via the persulfate anion may also occur (Liang and Su, 2009).

Fig. S10 (SI) displays the mass spectra for the byproduct detected under the reaction conditions at 55 °C. Butyric acid (BA) was the only byproduct detected, appearing between the 30 and 300 min reaction times. The concentration of BA was below the GC/MS limit of quantification. As shown in Fig. 1, 2-BE degradation slowed down compared to the degradation before 30 min. This suggest that BA, or the unidentified byproducts produced, compete with 2-BE for the radicals formed by persulfate. As observed by the TOC data in Fig. S6 at 55 °C, once BA is no longer detected after 300 min, TOC removal occurs more rapidly, suggesting that BA is more resistant to persulfate oxidation than the other byproducts produced. According to the TOC data, other reaction byproducts may exist, but were not detected with the available GC/MS methods. The increase in TOC removal after BA disappearance suggests that the subsequent byproducts breakdown more easily than BA.

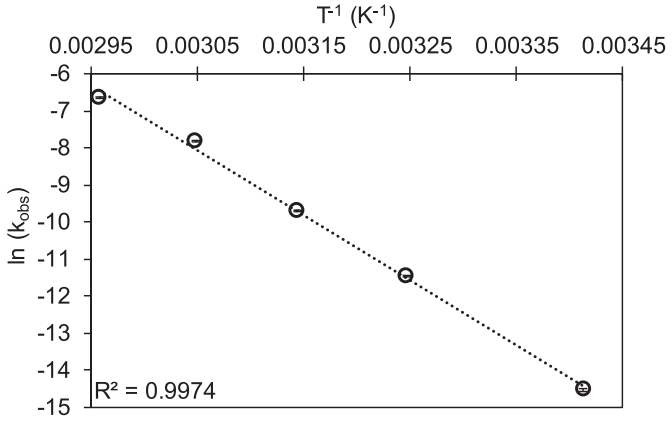

Fig. 2. Arrhenius plots for the oxidation of 2-BE by 21 mmol L^{-1} persulfate (initial pH 6, initial 2-BE concentration 120 mg L^{-1}). Error bars represent standard error.

3.2. pH effects

Fig. S11shows the decreasing 2-BE concentrations at initial pH 2, 6, and 11. The k_{obs} and half-live values are summarized in Table S2. Initial pH had little impact on 2-BE degradation. One-way ANOVA with Tukey's HSD post-hoc test was performed to evaluate differences in the mean pseudo-first-order reaction rate constants between the three pHs ($k_{obs,2\text{-}BE} = 3.061 \times 10^{-4}$ s^{-1} at pH 2, 4.074×10^{-4} s^{-1} at pH 6, 3.302×10^{-4} s^{-1} at pH 11). At the 95% confidence interval, the mean pseudo-first-order reaction rate constant at pH 6 is significantly different from the reaction rate constants at pH 2 and 11. However, the pseudo-first-order reaction rate at pH 2 and pH 11 are not significantly different from one another. Fig. S12 shows the TOC, pH and persulfate profiles for the reactions at all pHs. Over 480 min, 15% less TOC is degraded at pH 2 and 11 than at pH 6. At all three pHs, the same amount of persulfate was consumed. Thus, pH played little to no role in the degradation of 2-BE by persulfate at 55 °C.

At all pHs, the sulfate radical may react with water to produce a hydroxyl radical, as shown in Reaction 3 (Kolthoff and Miller, 1951; House, 1962; Herrmann et al., 1995). At alkaline pHs, the sulfate radical reacts with hydroxide to produce a hydroxyl radical and sulfate as shown in Reaction 3 (Liang and Su, 2009). However, at high temperatures the effect of pH on organic oxidation is less pronounced than at low temperatures (Ma et al., 2017; Manz and Carter, 2017). This suggest that the activation of persulfate at 55 °C according to Reaction 2 is a much faster than Reaction 4. Over the course of a fracture, pH may change as the fluids come in contact with the shale rock or as persulfate reactions occur. The data indicate that the higher temperatures, such as those observed in the well-bore, play a stronger role in the oxidation of 2-BE than the variation in pH over the course of a fracture would play.

$$SO_4^{\cdot -} + HO^- \rightarrow HO^{\cdot} + SO_4^{2-} \quad (4)$$

3.3. Iron (II) and shale effects

Fig. 3a displays decrease in 2-BE as Fe(II) is added to solution at 55 °C with an persulfate dose of 21 mmol L^{-1} (initial pH 2). The resulting $k_{obs,2\text{-}BE}$ and half-life values are summarized in Table S3. Control experiments showed that the addition of Fe(II) without persulfate did not cause 2-BE concentration to decrease in water, while persulfate addition and increasing Fe(II) concentrations increased the rate of 2-BE degradation (Kolthoff et al., 1951). The observed increase in 2-BE degradation is due to persulfate activation by Fe(II) that produces additional sulfate radicals, as shown in Reaction 5. To compare the resulting mean $k_{obs,2\text{-}BE}$ values, one-way ANOVA with Tukey's HSD post-hoc test was performed. The mean $k_{obs,2\text{-}BE}$ for 0 mg L^{-1} Fe(II) ($3.061 \times 10^{-4} s^{-1}$) was not statistically different from the mean rate constant for 5 mg L^{-1} Fe(II) ($3.360 \times 10^{-4} s^{-1}$) ($\alpha = 0.05$). The mean $k_{obs,2\text{-}BE}$ for 10 mg L^{-1} Fe(II) ($3.680 \times 10^{-4} s^{-1}$) was not statistically different from 5 nor 15 mg L^{-1} Fe(II) ($4.354 \times 10^{-4} s^{-1}$) ($\alpha = 0.05$). The mean $k_{obs,2\text{-}BE}$ values for 20 ($4.790 \times 10^{-4} s^{-1}$), 50 ($7.525 \times 10^{-4} s^{-1}$), and 100 ($1.130 \times 10^{-3} s^{-1}$), mg L^{-1} Fe(II) were significantly different from each other and all other tested Fe(II) concentrations ($\alpha = 0.05$). At

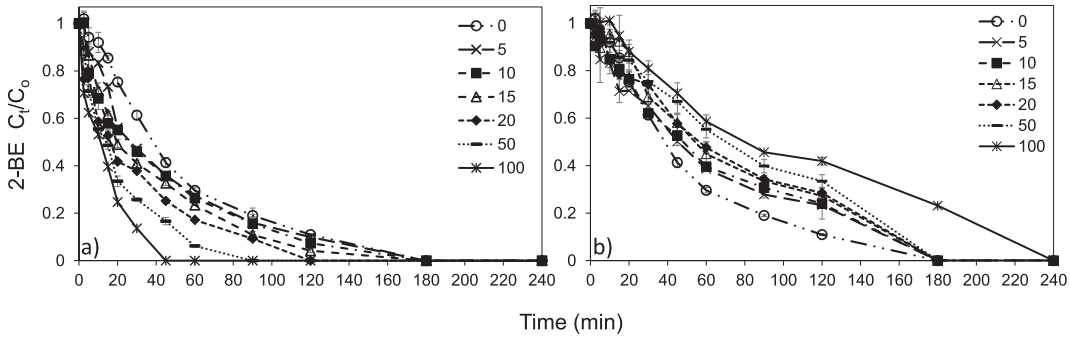

Fig. 3. Degradation of 2-BE in solutions with (a) Fe(II) and (b) shale rock (55 °C, initial dose of 21 mmol L^{-1} persulfate, initial pH 2, initial 2-BE concentration 120 mg L^{-1}). Legends indicate the mg L^{-1} concentration of Fe(II). Data below the limit of detection (0.957 mg L^{-1} 2-BE) were not used to calculate the rate constants reported in the text. Error bars represent standard error.

all iron concentrations, 2-BE was completely oxidized within 180 min at 55 °C. Fig. S13 displays the TOC, pH, and persulfate concentration profiles for the experiments with Fe(II) in solution (55 °C, persulfate dose of 21 mmol L^{-1}, initial pH 2). As expected, as more iron was added to solution, TOC and persulfate concentrations decreased at faster rates.

$$S_2O_8 + Me^{n+} \rightarrow SO_4^{-\cdot} + SO_4^{2-} + Me^{(n+1)+} \quad (5)$$

Fig. 3b displays the degradation of 2-BE when different concentrations of shale are in pH 2 solution (55 °C, 21 mmol L^{-1} persulfate). The concentration of shale added provides an iron concentration (0, 5, 10, 15, 20, 50, and 100 mg L^{-1}) comparable to the amounts tested in Fig. 3a. Table S4 summarizes the $k_{obs,2\text{-}BE}$ and half-live values for these reactions. Unlike Fe(II)-activation, increasing the iron concentration using shale did not lead to increasing $k_{obs,2\text{-}BE}$ values. When 18.86 mg L^{-1} of shale (5 mg L^{-1} Fe(II)) is added, completely 2-BE degradation is achieved after 180 min and the $k_{obs,2\text{-}BE}$ value is $2.477 \times 10^{-4} s^{-1}$. At the highest shale concentration tested, 373.6 mg L^{-1}, (100 mg L^{-1} Fe(II)) complete 2-BE degradation is achieved at 240 min and the $k_{obs,2\text{-}BE}$ value is $1.268 \times 10^{-4} s^{-1}$. As the shale concentration increases, the $k_{obs,2\text{-}BE}$ value decreases.

Fig. S14 shows persulfate profiles for the reactions with shale. At all shale concentrations, the persulfate concentration continues to decrease after complete degradation of 2-BE, as shown in Fig. S14. As shale concentration increases, the pseudo-first-order reaction rate constant decreases, despite the increasing iron concentration in the shale. In the field, pyrite dissolution and oxidation depends on dissolved oxygen content (Jew et al., 2017) and may vary compared to batch experiments. The decreasing pseudo-first-order reaction rate constant is due to the dissolution of other minerals in the shale, especially carbonates. Fig. 4 displays SEM images of the shale taken with a high definition back scatter detector (HDBSD), which allows for compositional and crystallographic information. Though the brighter spots in this image correspond to heavier elements, many were determined to be pyrite deposits. As displayed, the minerals in the shale used in this study are heterogeneously distributed throughout. When the shale is added to water or persulfate begins to react with the shale, these minerals dissolve into solution. The slower observed 2-BE degradation is due to the dissolution of these minerals, especially minerals like dolomite and calcite, which contain carbonate and can quench persulfate reactions (Tsitonaki et al., 2010). Fig. S15 displays the XRD pattern of the shale before and after the experiment. By comparing the XRD patterns before and after the experiment, observations may be made in how the reactions impacted the shale minerology. The two main minerals that were depleted from the shale are dolomite and calcite.

Carbonate speciation is dependent on pH, as shown in Reactions 6 and 7. In hydraulic fracturing conditions, such as those tested in this study, the pH of the injected fluids is as low as 2. Fig. S14 displays the change in pH over the course of the reactions with shale rock. In this study, the initial pH is 2 and does not change much over the course of the experiment. The amount of shale used is not enough to raise the pH, so the carbonates in solution are in the form of carbonic acid, H_2CO_3. The sulfate radical reacts with carbonic acid according to Reaction 8 (Criquet and Leitner, 2009) and the hydroxyl radical according to Reaction 9 (Czapski et al., 1999). The reaction occurs rapidly, consuming radicals in solution and preventing degradation of 2-BE. The carbonate radical produced in Reaction 8 and 9 may oxidize the remaining organics produced from 2-BE or inorganics from the shale, which would produce a carbonate anion (Neta et al., 1988).

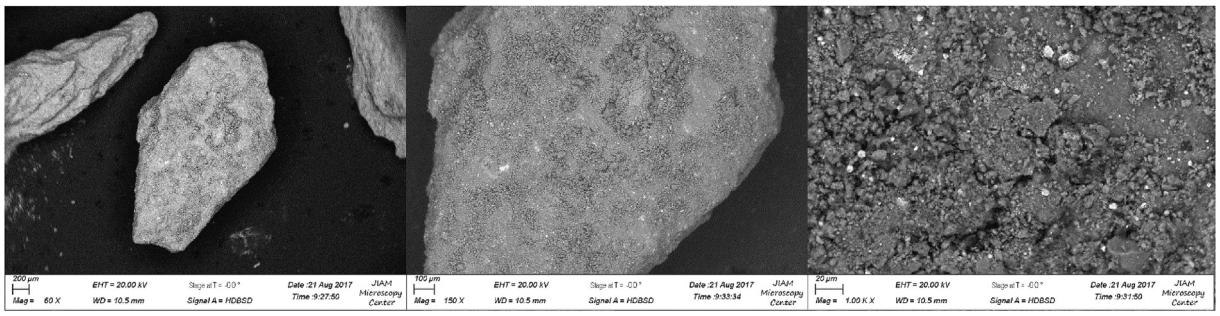

Fig. 4. Unreacted WV7 shale rock SEM images.

$$H_2CO_3 \rightarrow H^+ + HCO_3^-,\ pK_a = 6.3 \quad (6)$$

$$HCO_3^- \rightarrow H^+ + CO_3^{2-},\ pK_a = 10.3 \quad (7)$$

$$SO_4^{-\cdot} + H_2CO_3 \rightarrow CO_3^{-\cdot} + 2H^+ + SO_4^{2-},\ k \approx 10^6 M^{-1}s^{-1} \quad (8)$$

$$OH^{-\cdot} + H_2CO_3 \rightarrow CO_3^{-\cdot} + H_2O + H^+,\ k = 7.0 * 10^4\, M^{-1}s^{-1} \quad (9)$$

Persulfate may also react with other metals in the shale. Fig. 5 displays the major, minor, and trace metal dissolution into solution as 120 mg L^{-1} 2-BE and 21 mmol L^{-1} persulfate react with 373.6 mg L^{-1} shale (100 mg L^{-1} Fe(II)) in solution. As shown in Fig. 5, numerous metals increase in concentration as the reaction proceeds. Most metals constantly increase in concentration over the course of the reaction. Two metals, potassium and cesium, reach a maximum concentration after 90 min. While no cesium containing minerals were detected using XRD, cesium has been previously detected in flowback fluids (Lester et al., 2015) and typically occurs in pollucite, which is associated with minerals that naturally occur in shale (Freeborn et al., 1980), such as quartz and muscovite. Scaling metals, including calcium and magnesium, continually increase over the course of the reaction as displayed in Fig. 5. The calcium and magnesium are likely from the dolomite and calcite that are depleted from the shale as discussed earlier.

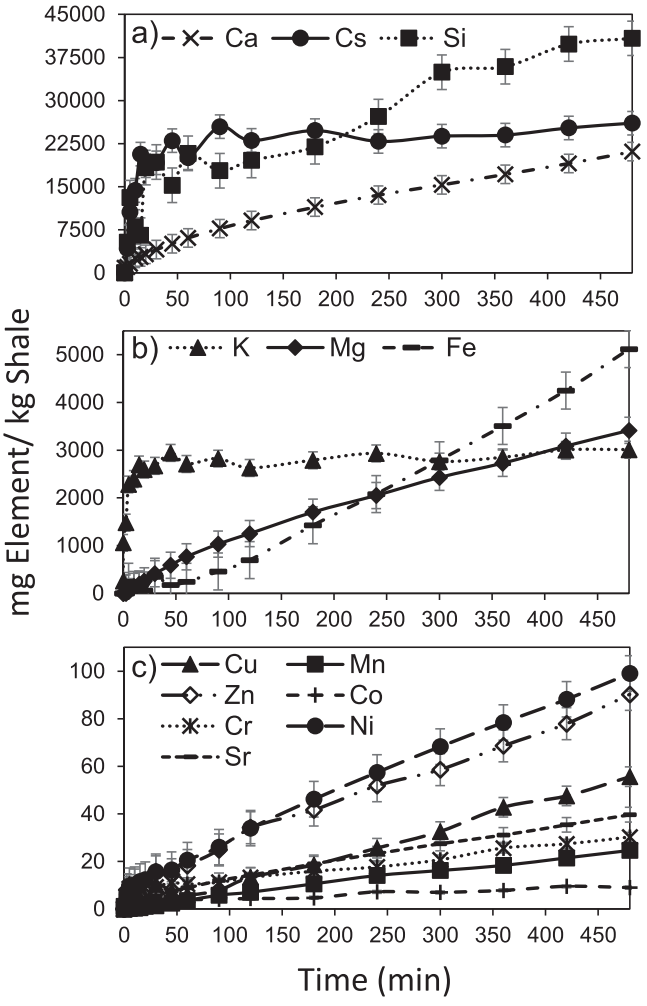

Fig. 5. Dissolution of (a) major, (b) minor, and (c) trace metals from the shale rock over the course of 2-BE degradation activated by 21 mmol L^{-1} persulfate (initial pH 2). Error bars represent standard error. Change in pH over the course of this reaction is displayed in Fig. S14.

In the field, the metal concentration detected in flowback and produced waters will depend on the amount of shale that the fluids come into contact with. This study shows that metals will precipitate into the fluids with minimal agitation. As soon as the shale was added to solution, metals began to precipitate. The exact metal concentrations in the field will vary depending on the shale play, the chemical supplier, and other factors. Additionally, 2-BE degradation was shown to slow in the presence of shale, which is likely due to the shale carbonate content. Further studies are needed to understand how individual additives contribute to the precipitation of metals from shale and how extreme pressures impact metal leaching.

4. Conclusion

In summary, the hydraulic fracturing spill indicator compound 2-BE may degrade readily downhole in the presence of activated persulfate. Conclusions from this study were:

- The persulfate anion may directly oxidize 2-BE at room temperature.
- As expected, increasing temperature sped up 2-BE degradation by persulfate activation due to the production of sulfate radicals.
- pH did not impact 2-BE degradation greatly.
- Increasing iron concentration increased the degradation rate of 2-BE; however, increasing the iron concentration using shale rock decrease the degradation rate.
- Metals continuously precipitate into solution during the oxidation reaction between 2-BE and persulfate. Further investigation is needed to understand how persulfate is impacting the dissolution of the minerals in the shale.

Acknowledgements

Funding for this project was provided by the University of Tennessee's Student/Faculty Research Award. The authors would like to acknowledge the University of Tennessee's and Oak Ridge National Laboratory's Joint Institute for Advanced Materials Microscopy Center and X-Ray Diffraction Core Facility for the use of their instruments. Thank you to Adrian Gonzalez at the University of Tennessee for his assistance with running ICP samples.

Appendix A. Supplementary data

Supplementary data related to this article can be found at https://doi.org/10.1016/j.chemosphere.2018.05.007.

References

Ahmad, M., Teel, A.L., Watts, R.J., 2010. Persulfate activation by subsurface minerals. J. Contam. Hydrol. 115, 34–45.
Czapski, G., Lymar, S.V., Schwarz, H.A., 1999. Acidity of the carbonate radical. J. Phys. Chem. 103, 3447–3450.
Chen, H., Carter, K.E., 2016. Water usage for natural gas production through hydraulic fracturing in the United States from 2008 to 2014. J. Environ. Manag. 170, 152–159.
Criquet, J., Leitner, N.K.V., 2009. Degradation of acetic acid with sulfate radical generated by persulfate ions photolysis. Chemosphere 77, 194–200.
DiGiulio, D.C., Jackson, R.B., 2016. Impact to underground sources of drinking water and domestic wells from production well stimulation and completion practices in the pavillion, Wyoming, field. Environ. Sci. Technol. 50, 4524–4536.
Ferrer, I., Thurman, E.M., 2015. Chemical constituents and analytical approaches for

hydraulic fracturing waters. Trend. Environ. Analytical Chem. 5, 18–25.
Freeborn, W.P., Zolensky, M., Scheetz, B.E., Komarneni, S., McCarthy, G.J., White, W.B., 1980. Shale Rocks as Nuclear Waste Repositories: Hydrothermal Reactions with Glass, Ceramic and Spent Fuel Waste Forms. Scientific Basis for Nuclear Waste Management. Springer, pp. 499–506.
Gaillard, N., Thomas, A., Favero, C., 2013. Novel Associative Acrylamide-based Polymers for Proppant Transport in Hydraulic Fracturing Fluids. Society of Petroleum Engineers.
Gregory, K.B., Vidic, R.D., Dzombak, D.A., 2011. Water management challenges associated with the production of shale gas by hydraulic fracturing. Elements 7, 181.
Grim, R.E., Rowland, R.A., 1944. Differential thermal analysis of clays and shales, a control and prospecting method*. J. Am. Ceram. Soc. 27, 65–76.
Herrmann, H., Reese, A., Zellner, R., 1995. Time-resolved UV/VIS diode array absorption spectroscopy of SOx−(x=3, 4, 5) radical anions in aqueous solution. J. Mol. Struct. 348, 183–186.
House, D.A., 1962. Kinetics and mechanism of oxidations by peroxydisulfate. Chem. Rev. 62, 185–203.
Jew, A.D., Dustin, M.K., Harrison, A.L., Joe-Wong, C.M., Thomas, D.L., Maher, K., Brown, G.E., Bargar, J.R., 2017. Impact of organics and carbonates on the oxidation and precipitation of iron during hydraulic fracturing of shale. Energy Fuel. 31, 3643–3658.
Kahrilas, G.A., Blotevogel, J., Corrin, E.R., Borch, T., 2016. Downhole transformation of the hydraulic fracturing fluid biocide glutaraldehyde: implications for flowback and produced water quality. Environ. Sci. Technol. 50, 11414–11423.
Kekacs, D., McHugh, M., Mouser, P.J., 2015. Temporal and thermal changes in density and viscosity of Marcellus shale produced waters. J. Environ. Eng. 141.
Kolthoff, I., Carr, E., 1953. Volumetric determination of persulfate in presence of organic substances. Anal. Chem. 25, 298–301.
Kolthoff, I.M., Medalia, A.I., Raaen, H.P., 1951. The reaction between ferrous iron and peroxides. IV. Reaction with potassium Persulfate1a. J. Am. Chem. Soc. 73, 1733–1739.
Kolthoff, I.M., Miller, I.K., 1951. The chemistry of persulfate. I. The kinetics and mechanism of the decomposition of the persulfate ion in aqueous Medium1. J. Am. Chem. Soc. 73, 3055–3059.
Lester, Y., Ferrer, I., Thurman, E.M., Sitterley, K.A., Korak, J.A., Aiken, G., Linden, K.G., 2015. Characterization of hydraulic fracturing flowback water in Colorado: implications for water treatment. Sci. Total Environ. 512, 637–644.
Liang, C., Huang, C.-F., Mohanty, N., Kurakalva, R.M., 2008. A rapid spectrophotometric determination of persulfate anion in ISCO. Chemosphere 73, 1540–1543.
Liang, C., Su, H.-W., 2009. Identification of sulfate and hydroxyl radicals in thermally activated persulfate. Ind. Eng. Chem. Res. 48, 5558–5562.
Liang, C., Wang, Z.-S., Mohanty, N., 2006. Influences of carbonate and chloride ions on persulfate oxidation of trichloroethylene at 20 °C. Sci. Total Environ. 370, 271–277.
Llewellyn, G.T., Dorman, F., Westland, J.L., Yoxtheimer, D., Grieve, P., Sowers, T., Humston-Fulmer, E., Brantley, S.L., 2015. Evaluating a groundwater supply contamination incident attributed to Marcellus Shale gas development. Proc. Natl. Acad. Sci. Unit. States Am. 112, 6325–6330.
Ma, J., Li, H., Chi, L., Chen, H., Chen, C., 2017. Changes in activation energy and kinetics of heat-activated persulfate oxidation of phenol in response to changes in pH and temperature. Chemosphere 189, 86–93.
Manz, K.E., Carter, K.E., 2016. Extraction and recovery of 2-butoxyethanol from aqueous phases containing high saline concentration. Analytical Chem. Research 9, 1–7.
Manz, K.E., Carter, K.E., 2017. Investigating the effects of heat activated persulfate on the degradation of furfural, a component of hydraulic fracturing fluid chemical additives. Chem. Eng. J. 327, 1021–1032.
Manz, K.E., Haerr, G., Lucchesi, J., Carter, K.E., 2016. Adsorption of hydraulic fracturing fluid components 2-butoxyethanol and furfural onto granular activated carbon and shale rock. Chemosphere 164, 585–592.
Marcon, V., Joseph, C., Carter, K.E., Hedges, S.W., Lopano, C.L., Guthrie, G.D., Hakala, J.A., 2017. Experimental insights into geochemical changes in hydraulically fractured Marcellus Shale. Appl. Geochem. 76, 36–50.
Minero, C., Maurino, V., Campanella, L., Morgja, C., Pelizzetti, E., 1989. Photodegradation of 2-ethoxy- and 2-butoxyethanol in the presence of semiconductor particles or organic conducting polymer. Environ. Technol. Lett. 10, 301–310.
Mouser, P.J., Borton, M., Darrah, T.H., Hartsock, A., Wrighton, K.C., 2016. Hydraulic fracturing offers view of microbial life in the deep terrestrial subsurface. FEMS (Fed. Eur. Microbiol. Soc.) 92 fiw166-fiw166.
Neta, P., Huie, R.E., Ross, A.B., 1988. Rate constants for reactions of inorganic radicals in aqueous solution. J. Phys. Chem. Ref. Data 17, 1027–1284.
Paukert Vankeuren, A.N., Hakala, J.A., Jarvis, K., Moore, J.E., 2017. Mineral reactions in shale gas reservoirs: barite scale formation from reusing produced water as hydraulic fracturing fluid. Environ. Sci. Technol. 51, 9391–9402.
Phan, T.T., Paukert Vankeuren, A.N., Alexandra Hakala, J., 2018. Role of water–rock interaction in the geochemical evolution of Marcellus Shale produced waters. Int. J. Coal Geol.
Rogers, J.D., Burke, T.L., Osborn, S.G., Ryan, J.N., 2015. A framework for identifying organic compounds of concern in hydraulic fracturing fluids based on their mobility and persistence in groundwater. Environ. Sci. Technol. Lett. 2, 158–164.
Rogers, J.D., Ferrer, I., Tummings, S.S., Bielefeldt, A.R., Ryan, J.N., 2017. Inhibition of biodegradation of hydraulic fracturing compounds by glutaraldehyde: groundwater column and microcosm experiments. Environ. Sci. Technol. 51, 10251–10261.
Stringfellow, W.T., Domen, J.K., Camarillo, M.K., Sandelin, W.L., Borglin, S., 2014. Physical, chemical, and biological characteristics of compounds used in hydraulic fracturing. J. Hazard Mater. 275, 37–54.
Thurman, E.M., Ferrer, I., Blotevogel, J., Borch, T., 2014. Analysis of hydraulic fracturing flowback and produced waters using accurate mass: identification of ethoxylated surfactants. Anal. Chem. 86, 9653–9661.
Torres, L., Yadav, O.P., Khan, E., 2016. A review on risk assessment techniques for hydraulic fracturing water and produced water management implemented in onshore unconventional oil and gas production. Sci. Total Environ. 539, 478–493.
Tsitonaki, A., Petri, B., Crimi, M., MosbÆK, H., Siegrist, R.L., Bjerg, P.L., 2010. Situ chemical oxidation of contaminated soil and groundwater using persulfate: a review. Crit. Rev. Environ. Sci. Technol. 40, 55–91.